View metadata, citation and similar papers at core.ac.uk

brought to you by CORE

provided by Dominican Scholar

DOMINICAN UNIVERSITY of CALIFORNIA

Dominican Scholar

Natural Sciences and Mathematics | Faculty Scholarship

Department of Natural Sciences and Mathematics

7-17-2018

Antimalarial proteasome inhibitor reveals collateral sensitivity from intersubunit interactions and fitness cost of resistance.

Laura A. Kirkman
Division of Infectious Diseases, Department of Medicine, Weill Cornell Medicine

Wenhu Zhan
Department of Microbiology and Immunology, Weill Cornell Medicine

Joseph Visone
Division of Infectious Diseases, Department of Medicine, Weill Cornell Medicine

Alexis Dziedziech
Division of Infectious Diseases, Department of Medicine, Weill Cornell Medicine

Pradeep K. Singh
Chemical Core Facility, Department of Biochemistry, Weill Cornell Medicine

Survey: Let us know how this paper benefits you.

See next page for additional authors

Recommended Citation

Kirkman, Laura A.; Zhan, Wenhu; Visone, Joseph; Dziedziech, Alexis; Singh, Pradeep K.; Fan, Hao; Tong, Xinran; Bruzual, Igor; Hara, Ryoma; Kawasaki, Masanori; Imaeda, Toshihiro; Okamoto, Rei; Sato, Kenjiro; Michino, Mayako; Alvaro, Elena Fernandez; Guiang, Liselle F.; Sanz, Laura; Mota, Daniel J.; Govindasamy, Kavitha; Wang, Rong; Ling, Yan; Tumwebaze, Patrick K.; Sukenick, George; Shi, Lei; Vendome, Jeremie; Bhanot, Purnima; Rosenthal, Philip J.; Aso, Kazuyoshi; Foley, Michael A.; Cooper, Roland A.; Kafsack, Bjorn; Doggett, J Stone; Nathan, Carl F.; and Lin, Gang, "Antimalarial proteasome inhibitor reveals collateral sensitivity from intersubunit interactions and fitness cost of resistance." (2018). *Natural Sciences and Mathematics | Faculty Scholarship*. 38.
https://doi.org/10.1073/pnas.1806109115

https://doi.org/10.1073/pnas.1806109115

This Article is brought to you for free and open access by the Department of Natural Sciences and Mathematics at Dominican Scholar. It has been accepted for inclusion in Natural Sciences and Mathematics | Faculty Scholarship by an authorized administrator of Dominican Scholar. For more information, please contact michael.pujals@dominican.edu.

Authors

Laura A. Kirkman, Wenhu Zhan, Joseph Visone, Alexis Dziedziech, Pradeep K. Singh, Hao Fan, Xinran Tong, Igor Bruzual, Ryoma Hara, Masanori Kawasaki, Toshihiro Imaeda, Rei Okamoto, Kenjiro Sato, Mayako Michino, Elena Fernandez Alvaro, Liselle F. Guiang, Laura Sanz, Daniel J. Mota, Kavitha Govindasamy, Rong Wang, Yan Ling, Patrick K. Tumwebaze, George Sukenick, Lei Shi, Jeremie Vendome, Purnima Bhanot, Philip J. Rosenthal, Kazuyoshi Aso, Michael A. Foley, Roland A. Cooper, Bjorn Kafsack, J Stone Doggett, Carl F. Nathan, and Gang Lin

This article is available at Dominican Scholar: https://scholar.dominican.edu/natural-sciences-and-mathematics-faculty-scholarship/38

Antimalarial proteasome inhibitor reveals collateral sensitivity from intersubunit interactions and fitness cost of resistance

Laura A. Kirkman[a,b,1], Wenhu Zhan[b,2], Joseph Visone[a,2], Alexis Dziedziech[a], Pradeep K. Singh[c], Hao Fan[b], Xinran Tong[b], Igor Bruzual[d], Ryoma Hara[e], Masanori Kawasaki[e], Toshihiro Imaeda[e], Rei Okamoto[e], Kenjiro Sato[e], Mayako Michino[e], Elena Fernandez Alvaro[f], Liselle F. Guiang[g], Laura Sanz[f], Daniel J. Mota[h], Kavitha Govindasamy[i], Rong Wang[j], Yan Ling[b], Patrick K. Tumwebaze[k], George Sukenick[j], Lei Shi[l], Jeremie Vendome[m], Purnima Bhanot[i], Philip J. Rosenthal[h], Kazuyoshi Aso[e], Michael A. Foley[e], Roland A. Cooper[g], Bjorn Kafsack[b], J. Stone Doggett[d], Carl F. Nathan[b,1], and Gang Lin[b,1]

[a]Division of Infectious Diseases, Department of Medicine, Weill Cornell Medicine, NY 10065; [b]Department of Microbiology and Immunology, Weill Cornell Medicine, NY 10065; [c]Chemical Core Facility, Department of Biochemistry, Weill Cornell Medicine, NY 10065; [d]Department of Research and Development, Portland Veterans Affairs Medical Center, Oregon Health and Science University, Portland, OR 97239; [e]Tri-Institutional Therapeutics Discovery Institute, New York, NY 10065; [f]Diseases of the Developing World (DDW), Tres Cantos Medicine Development Campus, GlaxoSmithKline, Severo Ochoa 2, 28760, Tres Cantos, Madrid, Spain; [g]Department of Natural Sciences and Mathematics, Dominican University of California, San Rafael, CA 94901; [h]Department of Medicine, University of California, San Francisco, CA 94143; [i]Department of Microbiology, Biochemistry and Molecular Genetics, Rutgers New Jersey Medical School, Newark, NJ 11201; [j]NMR Analytical Core Facility, Memorial Sloan Kettering Cancer Center, New York, NY 10065; [k]Infectious Diseases Research Collaboration, Kampala, Uganda; [l]Department of Biophysics, Weill Cornell Medicine, NY 10065; and [m]Schrödinger, Inc., New York, NY 10036

Contributed by Carl F. Nathan, June 10, 2018 (sent for review April 9, 2018; reviewed by Peter Agre and Thomas E. Wellems)

We describe noncovalent, reversible asparagine ethylenediamine (AsnEDA) inhibitors of the *Plasmodium falciparum* proteasome (Pf20S) β5 subunit that spare all active subunits of human constitutive and immuno-proteasomes. The compounds are active against erythrocytic, sexual, and liver-stage parasites, against parasites resistant to current antimalarials, and against *P. falciparum* strains from patients in Africa. The β5 inhibitors synergize with a β2 inhibitor in vitro and in mice and with artemisinin. *P. falciparum* selected for resistance to an AsnEDA β5 inhibitor surprisingly harbored a point mutation in the noncatalytic β6 subunit. The β6 mutant was resistant to the species-selective Pf20S β5 inhibitor but remained sensitive to the species-nonselective β5 inhibitors bortezomib and carfilzomib. Moreover, resistance to the Pf20S β5 inhibitor was accompanied by increased sensitivity to a Pf20S β2 inhibitor. Finally, the β5 inhibitor-resistant mutant had a fitness cost that was exacerbated by irradiation. Thus, used in combination, multistage-active inhibitors of the Pf20S β5 and β2 subunits afford synergistic antimalarial activity with a potential to delay the emergence of resistance to artemisinins and each other.

Plasmodium | malaria | proteasome inhibitors | artemisinin | collateral sensitivity

Each year malaria causes an estimated 200 million cases and nearly 500,000 deaths in children under 5 y of age, with the large majority of serious illnesses and deaths due to *Plasmodium falciparum* (1). Resistance to older antimalarials, such as chloroquine, is common, and resistance to the most effective newer treatments, artemisinin-based combination therapies (ACTs), is established in Southeast Asia (2–4). Compounds that target the preerythrocytic hepatic stage and block the development of the transmissible gametocyte form that are taken up by the mosquito are ideal candidates for malaria prevention, but few antimalarials are effective against these stages. The growing threat of ACT failure and the need to target nonerythrocytic stages underscore the need for drugs with new targets in the parasite.

Proteasome inhibitors have the potential to fulfill both requirements (5), and the proteasome has emerged as an important target for antimalarial drug development (6–10). Eukaryotic proteasomes have two copies of each of the three proteolytically active subunits—chymotryptic β5, tryptic β2, and caspase-like β1—in each 20S core particle. Several proteasome inhibitors are effective in vitro against *Plasmodium* spp. at multiple stages of the parasite lifecycle, including the erythrocytic, liver, and gametocyte stages, and for the treatment of *Plasmodium berghei*-infected mice (9, 11–15). The human host has two major isoforms of the 20S, constitutive proteasomes (c-20S) and immunoproteasomes (i-20S), with subtle but significant differences in proteolytic activity and functions. Proteasomes are important in all human cells. Inhibition of c-20S is cytotoxic, and inhibition of i-20S can dampen immune responses against infection (16, 17). Proteasome inhibitors designed to treat infections must achieve a high degree of species

Significance

Protozoal proteasome is a validated target for antimalarial drug development, but species selectivity of reported inhibitors is suboptimal. Here we identify inhibitors with improved selectivity for malaria proteasome β5 subunit over each active subunit of human proteasomes. These compounds kill the parasite in each stage of its life cycle. They interact synergistically with a β2 inhibitor and with artemisinin. Resistance to the β5 inhibitor arose through a point mutation in the nonproteolytic β6 subunit. The same mutation made the mutant strain more sensitive to a β2 inhibitor and less fit to withstand irradiation. These findings reveal complex interplay among proteasome subunits and introduce the prospect that combined inhibition of β2 and β5 subunits can afford synergy and thwart resistance.

Author contributions: L.A.K., C.F.N., and G.L. designed research; L.A.K., W.Z., J. Visone, A.D., P.K.S., H.F., X.T., I.B., R.H., M.K., T.I., R.O., K.S., M.M., E.F.A., L.F.G., L. Sanz, D.J.M., K.G., R.W., Y.L., P.K.T., L. Shi, J. Vendome, P.B., R.A.C., B.K., J.S.D., and G.L. performed research; P.K.S., R.H., M.K., T.I., R.O., K.S., K.A., B.K., and G.L. contributed new reagents/analytic tools; L.A.K., W.Z., J. Visone, A.D., H.F., X.T., I.B., R.H., M.K., T.I., R.O., K.S., M.M., E.F.A., L.F.G., L. Sanz, D.J.M., K.G., R.W., P.K.T., G.S., L. Shi, J. Vendome, P.B., P.J.R., K.A., M.A.F., R.A.C., B.K., J.S.D., and G.L. analyzed data; and L.A.K., C.F.N., and G.L. wrote the paper.

Reviewers: P.A., Johns Hopkins Bloomberg School of Public Health; and T.E.W., National Institutes of Health.

The authors declare no conflict of interest.

This open access article is distributed under Creative Commons Attribution-NonCommercial-NoDerivatives License 4.0 (CC BY-NC-ND).

[1]To whom correspondence may be addressed. Email: lak9015@med.cornell.edu, cnathan@med.cornell.edu, or gal2005@med.cornell.edu.

[2]W.Z. and J.V. contributed equally to this work.

This article contains supporting information online at www.pnas.org/lookup/suppl/doi:10.1073/pnas.1806109115/-/DCSupplemental.

Published online July 2, 2018.

selectivity to avoid toxicity and impairment of the host's immune response.

Developing pathogen-selective proteasome inhibitors that spare both i-20S and c-20S has been challenging, as proteasome subunits are highly conserved. Species-selective proteasome inhibitors were first reported for *Mycobacterium tuberculosis* (18, 19) and then for *Plasmodium sp* (6, 10), trypanosomes and Leishmania (20). However, most studies confined assessment of selectivity to testing the impact of these compounds on host c-20S, whereas i-20S inhibition was not examined. Moreover, most studies tested activity against only one of the human proteasome subunits.

Here we present a class of proteasome inhibitors that is highly species-selective for the Pf20S β5 subunit over all active subunits of both human c-20S and i-20S. Use of these inhibitors revealed three previously unreported findings with Pf20S inhibition: late-stage gametocytocidal activity and inhibition of gamete activation; marked synergy between a Pf20S β5 inhibitor and a β2 inhibitor; and association of resistance to a Pf20S β5 inhibitor with markedly increased sensitivity to inhibition of β2. The findings of synergy and collateral sensitivity suggest the potential value of capitalizing on interactions among different subunits of the parasite proteasome.

Results

Identification of Antimalarial Asparagine Ethylenediamines. A focused proteasome inhibitor library of around 180 compounds including three unique classes was synthesized in-house (18, 19, 21–24). We randomly selected 95 of these compounds at 10 μM with bortezomib, a pan-proteasome inhibitor, serving as a positive control (Fig. 1*A*). Initial screens measured the ability of the compound to inhibit hydrolysis of a fluorogenic chymotryptic substrate, suc-Leu-Leu-Val-Tyr (LLVY)-AMC, by a *P. falciparum* lysate. We focused further on compounds that afforded >85% inhibition of suc-LLVY-AMC hydrolysis, comparable to the impact of bortezomib. We next tested compounds against the erythrocytic stage of the parasite using a standard in vitro growth inhibition assay over 72 h (Fig. 1*D*) (25). Compounds in classes of N,C-capped dipeptides (22) and β-amino acid dipeptidomimetics (23) were potent against *P. falciparum* but were also potent inhibitors of i-20S and hence were not sufficiently species selective. We next focused on compounds belonging to a recently reported class of proteasome inhibitors, the asparagine ethylenediamines (AsnEDAs) (17). Among these, PKS3080 and PKS21004 showed the most potent antimalarial activity (Fig. 1*A* and *SI Appendix*, Table S1). PKS21003, a regioisomer of PKS21004, was inactive against the parasite and served as a negative control.

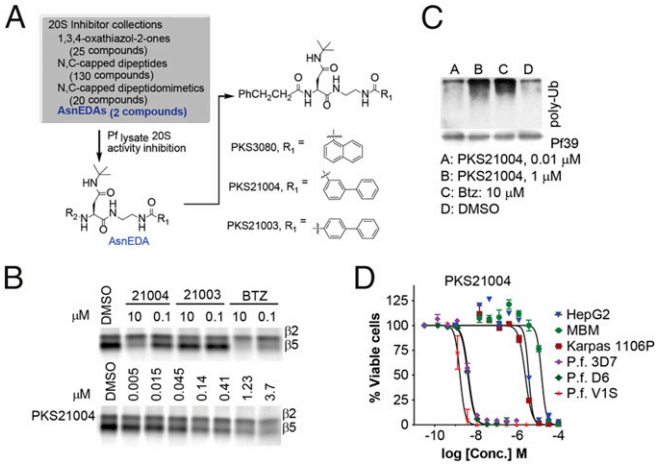

Fig. 1. Identification of AsnEDA Pf20S inhibitors and their characterization. (*A*) Screening cascade to identify PKS3080, 21004, and the inactive congener PKS21003. (*B*) Inhibition of *P. falciparum* cell-free lysates by PKS21004 and bortezomib (BTZ), and dose-dependent inhibition by PKS21004 as assessed by activity-based probe MV151. (*C*) PKS21004-dependent accumulation of polyubiquinated proteins in parasites. (*D*) Growth inhibition of PKS21004 against three *P. falciparum* strains and cytotoxicity against three types of mammalian cells; data shown are the average of three independent experiments, each performed in triplicate.

We assessed subunit selectivity with the activity-based proteasome probe MV151, a fluorescent vinyl sulfone that irreversibly labels the three catalytic subunits of the parasite proteasome (7, 26). PKS21004 and bortezomib specifically inhibited labeling of Pf20S β5, whereas PKS21003 did not (Fig. 1*B*, *Upper*). In contrast, PKS21004 did not block MV151 from labeling Pf20S β2 or β1. Importantly, none of the AsnEDAs showed appreciable inhibitory activity against the human c-20S subunits β1c or β2c or the i-20S subunits β1i or β2i (17). In contrast, in our assay, Trp-Leu-Trp-vinyl sulfone (WLW-VS) (6), reported to be highly selective for Pf20S β2 over human c-20S β2c and human i-20S β2i, was highly potent against human c-20S β5c and human i-20S β5i, with IC_{50}s of 100 nM and 23 nM, respectively (*SI Appendix*, Fig. S1). Thus, it is important to confirm species selectivity by testing all proteasome subunits, as inhibitors intended for one subunit of one species can inhibit different subunits of a different species.

The ability of PKS21004 to block the covalent reaction with Pf20S β5 and MV151 was dose-dependent (Fig. 1*B*, *Lower*). Polyubiquitinylated proteins accumulated in *P. falciparum* (Pf3D7 strain) in vitro within 4 h of exposure to 1 μM PKS21004, similar to results with 10 μM bortezomib (Fig. 1*C*).

We tested the cytotoxicity of PKS21004 and PKS21003 against the human hepatoma cell line HepG2, which predominantly expresses c-20S, the human lymphoma cell line Karpas 1106P, which predominantly expresses i-20S, and primary mouse bone marrow-derived macrophages (MBM), which also express i-20S. PKS21004 was selectively toxic for *P. falciparum* over the mammalian cells, while PKS21003 was nontoxic for both *P. falciparum* and mammalian cells (Fig. 1*D* and *SI Appendix*, Table S1).

Docking and Structure–Activity Relationship Studies to Improve Species Selectivity. To guide structure–activity (SAR) studies, we modeled the binding mode of PKS21004 in Pf20S, based on the recently solved cryo-electron microscopy structure of PKS21004 bound to i-20S (17). Given the high sequence and structural similarity between human i-20S and Pf20S for the relevant β5 and β6 subunits (~60% sequence similarity and ~1.1-Å rmsd for the dimers' Cαs), we predicted that the binding mode of PKS21004 in Pf20S would be similar to that in i-20S. In i-20S β5iβ6 (Fig. 2*A*), the biphenyl moiety of PKS21004 binds to the S1 pocket and S1 side pocket, while the Asn(*t*-butyl) binds to the S3 pocket, forming hydrogen bonds with Ser27 and Ser129 of β5i. N-capped phenylpropionate of the inhibitor binds to S4, a solvent-exposed pocket formed by amino acid residues of β6 (17). In Pf20S β5β6, PKS21004 is predicted to form very similar interactions with the S1, S3, and S4 pockets (Fig. 2*B* and *SI Appendix*, Fig. S2).

Using this model, we conducted SAR studies and developed the species-selective Pf20S inhibitors PKS21224 and PKS21287 (Fig. 2*C*) by replacing the biphenyl of PKS21004 with heteroaromatic rings (PKS21208 and PKS21229) and by replacing the tosyl with a hydrophilic isoxazolyl carboxamide. Both compounds were highly potent and modestly selective for Pf20S over c-20S and i-20S (Fig. 2*F*). All compounds were highly active against *P. falciparum* and selective against parasite versus HepG2 cells. PKS21224 and PKS21287, which both have lower logD (the log of the partition of a chemical compound between the lipid and aqueous phases) than PKS21004, were the least active against i-20S and c-20S but were highly potent against *P. falciparum*, with EC_{50}s of 9 nM and 34 nM, respectively. However, PKS21287 had poor cell permeability in a parallel artificial membrane permeability assay (*SI Appendix*, Table S2). We therefore modified the pyrazole moiety by changing the C–C linker to a C–N linker,

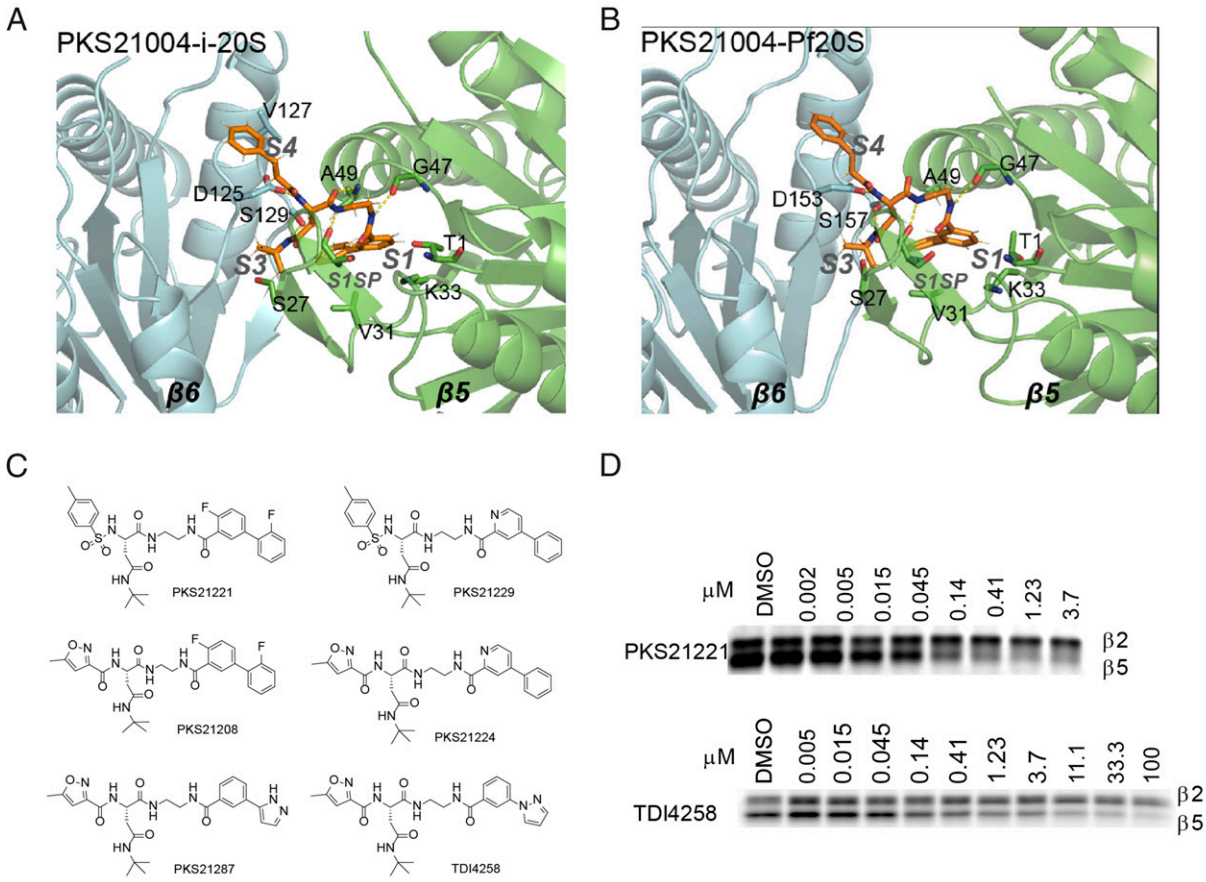

E

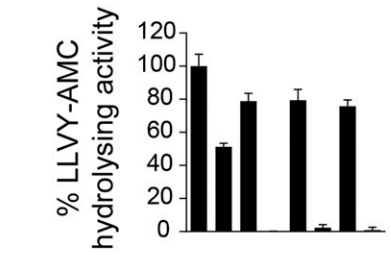

DMSO	+	-	-	-	-	-	-	-
WLW-VS (0.5 μM)	-	+	-	+	-	+	-	+
PKS21004(10 μM)	-	-	+	+	-	-	-	-
TDI4258 (10μM)	-	-	-	-	+	+	-	-
PKS21221 (10μM)	-	-	-	-	-	-	+	+

F

IC50s of proteasome inhibitors versus hu20S β5i, β5c and Pf20S and their EC50s against P. falciparum and HepG2

ID	IC50 (nM)			SI		EC50 (nM)		SI
	β5i	β5c	Pf20S	β5i / Pf20S	β5c / Pf20S	Pf 3D7	HepG2	
PKS21004	58	326	3.1	19	105	4.6	3670	798
PKS21221	4	110	3.8	1.1	28	1.56	1690	>3,000
PKS21208	24	1,130	5.2	5	217	1.7	69,000	40,000
PKS21229	19	530	2.3	8	230	1	8,800	8,800
PKS21224	746	33,740	57.3	13	588	9	136,000	>15,000
PKS21287	1,150	21,060	114.7	10	184	34	> 100,000	> 2,940
TDI4258	780	10,110	58.5	13	173	29	> 100,000	> 3,400

Data were average of at least 3 independent experiments.

Fig. 2. AsnEDAs with improved potency and selectivity. (*A* and *B*) Binding mode of PKS21004 in the i-20S structure (17) (*A*) and in Pf20S (*B*) predicted by docking. Only β5 and β6 are shown. Key amino acid residues involved in ligand binding are labeled in the respective enzymes. (*C*) Structures of AsnEDAs. (*D*) Dose-dependent inhibition of Pf20S by PKS21221 and by TDI4258 assessed by the activity-based probe MV151. (*E*) LLVY-AMC hydrolysis by Pf20S was assessed in the presence of AsnEDAs and WLW-VS, both separately and in combination. (*F*) IC_{50}s of all AsnEDAs against human i-20S, c-20S, and Pf20S and EC_{50}s against *P. falciparum* 3D7 and HepG2. All data are averages of at least three independent experiments.

resulting in TDI4258. PKS21287 and TDI4258 showed comparable IC_{50}s against c-20S and i-20S and EC_{50}s against *P. falciparum* 3D7 (Fig. 2*F*). The logD of TDI4258 at pH 7.4 (1.85) was greater than that of PKS21287 (1.49). The change was associated with an improvement in permeability from an undetectable level for PKS21287 to 64 nm/s at pH 7.4 and 56 nm/s at pH 5.0 for TDI4258. However, only 2.3% of an orally administered dose of TDI4258 was bioavailable. Consistent with their reduced inhibitory activity against human proteasomes, PKS21224, PKS21287, and TDI4258 were much less cytotoxic to mammalian cells than PKS21004 and PKS21221 (Fig. 2*F*). As expected, PKS21221 and TDI4258 dose-dependently blocked the labeling of Pf20S β5 by MV151 (Fig. 2*D*).

Determination of IC_{50}s Against Pf20S β5. Using purified Pf20S, we observed that hydrolysis of substrate suc-LLVY-AMC was reduced by 20–30% in the presence of the β5-specific inhibitors PKS21004, PKS21221, or TDI4258 at 10 μM and by 50% by the β2-specific inhibitor WLW-VS at 0.5 μM (Fig. 2*E*) (6). This suggested that both β2 and β5 of the Pf20S can hydrolyze

A

IC50s of PKS21004 and PKS21003 against P. falciparum strains

P. f. Strain	Phenotype	EC50 (nM)	
		PKS21004	PKS21003
3D7	SUL – R	0.0046	> 2.77
HB3	PYR – R	0.010	> 2.77
D6	Pan – S	0.004	> 2.77
Sb1-a6	ATOV – R	0.0048	> 2.77
Dd2	MDR	0.0048	> 2.77
V1S	MDR	0.0017	> 2.77
IPC 3663	ART – S	0.006	> 2.77
IPC 5188	ART – S	0.0015	> 2.77
IPC 4884	ART – R	0.0052	> 2.77
IPC 5202	ART – R	0.0046	NT
IPC 4912	ART – R	0.0058	NT

ART: artemisinin; ATOV: Atovaquone; MDR: multi-drug resistant; PYR: pyrimethamine; R: resistant; S: sensitive; SUL: sulfadoxine;

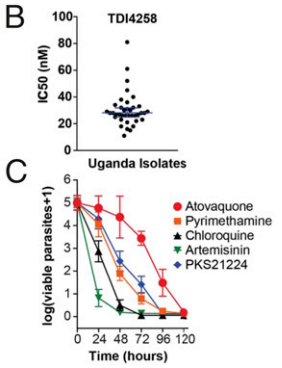

Fig. 3. Erythrocytic stage and ex vivo activities and PRR of AsnEDAs. (*A*) IC_{50}s of PKS21004 against various strains of *P. falciparum*. (*B*) Ex vivo activity of TDI4258 against 38 clinical samples of isolates from Uganda. The geometric mean EC_{50} was calculated as 30 nM. (*C*) PRR of PKS21224. An in vitro parasite reduction rate assay was used to determine onset of action and rate of killing as described (28). *P. falciparum* was exposed to PKS21224 at a concentration equivalent to 10× EC_{50}. The number of viable parasites at each time point was determined as described. Four independent serial dilutions were done with each sample to correct for experimental variation; error bars indicate SD. Previous results with current antimalarial drugs tested using the same protocol are shown for comparison (28).

suc-LLVY-AMC. The combination of WLW-VS at 0.5 μM and any of the AsnEDA inhibitors at 10 μM reduced suc-LLVY-AMC hydrolysis by >95%, implying synergy between β2 and β5 inhibition of enzymatic activities. We determined the IC_{50}s of our compounds against Pf20S β5 in the presence of 0.5 μM WLW-VS in enzymatic screens to block the confounding hydrolysis by β2 (Fig. 2*F*). We improved the selectivity indexes of AsnEDAs for Pf20S versus human c-20S (Fig. 2*F*) from 28-fold for PKS21221 to 588-fold for PKS21224 and increased the IC_{50}s against i-20S β5i by 280-fold (from 4 nM to 1,150 nM) with only an approximately sixfold reduction in EC_{50}s in a whole-cell assay. The IC_{50}s of all tested compounds correlated well with their respective EC_{50}s against *P falciparum* in vitro (*SI Appendix*, Fig. S3).

Activity Against the Asexual Erythrocytic Stage. We next determined the EC_{50}s of PKS21004 against established laboratory strains of *P. falciparum* with different points of origin and with different drug-resistance profiles (Fig. 3*A*). PKS21004 was potent against all lines tested. EC_{50}s ranged from 1.5 nM against *P. falciparum* V1S, a multidrug-resistant South East Asian strain, to 10 nM against *P. falciparum* HB3, a Central American strain resistant to pyrimethamine. Five more recently isolated parasite strains from the Greater Mekong subregion, two of which are artemisinin sensitive and three of which are artemisinin resistant, showed a narrow range of EC_{50}s (1.5 nM–6 nM) to PKS21004. PKS21221, PKS21287, and PKS21224 also showed activity (*SI Appendix*, Fig. S4).

TDI4258 was further tested for ex vivo activity against *P. falciparum* samples from 38 malaria patients in Uganda. The EC_{50}s ranged from 11–81 nM, with a mean of 30 nM (Fig. 3*B* and *SI Appendix*, Table S3), which is consistent with EC_{50}s against the *P. falciparum* laboratory strains. There was no detectable association between sensitivities to TDI4258 and chloroquine among the tested Ugandan isolates (*SI Appendix*, Table S3) (27).

To understand the dynamics of antimalarial action, we assessed the in vitro killing profile of PKS21224. The in vitro parasite reduction ratio (PRR) assay directly measures the number of parasites that remain viable at different time points post drug exposure (28). PKS21224 showed a *P. falciparum* killing profile similar to that of pyrimethamine (log PRRs of 2.7 and 2.8, respectively) (Fig. 3*C*) with a lag phase (the time needed to observe the maximal killing effects of the drug) of 24 h and a parasite clearance time (the time needed to kill 99.9% of the initial population) of 61 h.

Activity Against *P. falciparum* Transmission and Mosquito Stages. We tested activities of PKS21004, PKS21224, and PKS21287 against stage III (Fig. 4*A*) and stage V *P. falciparum* gametocytes with dihydroartemisinin (DHA) as a positive control (Fig. 4*B*). All three compounds showed in vitro antigametocyte activity after 24, 48, and 72 h, with EC_{50}s of 28, 140, and 212 nM, respectively. Antigametocyte activity increased by 2.3- to 3.6-fold from 24 to 48 h (*SI Appendix*, Fig. S5 and Table S4) with little additional enhancement of killing at 72 h. In comparison, the activity of DHA did not improve with exposure longer than 24 h, consistent with its rapid killing mechanism. Our compounds were also effective against mature stage V gametocytes at 72 h, with EC_{50}s of 57 nM, 227 nM, and 229 nM for PKS21004, PKS21224, and PKS21287, respectively (Fig. 4*B*).

PKS21224, PKS21287, and TDI4258 were further tested in a gamete activation assay. The activation of male but not female gametes was susceptible to inhibition of Pf20S β5, with EC_{50}s of 140 nM–240 nM (Fig. 4*C* and *SI Appendix*, Table S5) (29). The inability of male gametes to undergo activation would preclude the generation of infectious sporozoites and block malaria transmission.

Activity Against Hepatic-Stage Parasites. The activity of PKS21004 against preerythrocytic-stage parasites was tested using a *P. berghei*-HepG2 model. Luciferase-expressing *P. berghei* sporozoites were added to HepG2 cells in the presence or absence of PKS21004 (30). Infectivity was determined 48 h postinfection by quantification of luciferase activity. PKS21004 demonstrated potent inhibition of liver-stage development with an EC_{50} of 16.3 nM (Fig. 4*D*). Due to the selectivity of our compounds, we were able to determine the effect of proteasome inhibition directly on sporozoite-to-merosome development before and after hepatic cell invasion. Our findings

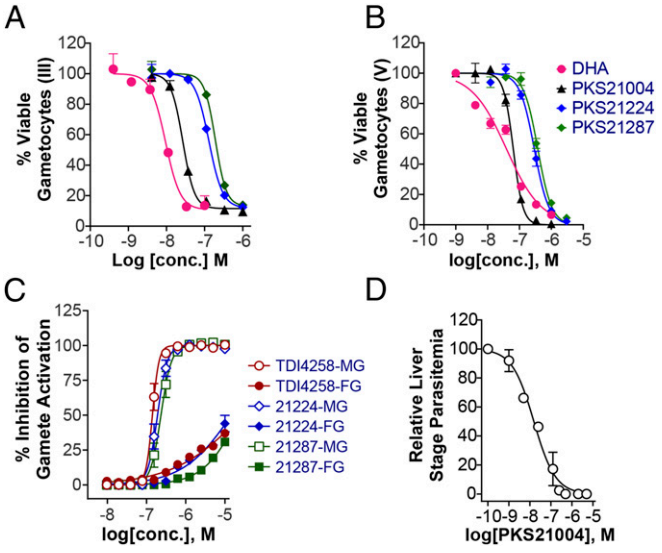

Fig. 4. Antimalarial activities of AsnEDAs against gametocyte stage, gamete activation, and liver stage. (*A* and *B*) AsnEDAs and DHA as a positive control were dose-dependently evaluated against gametocytes at stages III (*A*) and V (*B*). (*C*) Inhibition of *P. falciparum* gamete activation. PKS21224, PKS21287, and TDI4258 were dose-dependently evaluated in a dual gamete activation assay. FG, female gametes; MG, male gametes. (*D*) Dose–response curve of PKS21004s activity against *P. berghei* preerythrocytic stages in the HepG2 model. Data shown are the average of three independent experiments, each performed in triplicate.

suggest that functional proteasomes are required for parasite development within the hepatocyte.

Synergy Between DHA and Proteasome Inhibitors. Parasite proteasome inhibition reportedly can reverse artemisinin resistance (5), where artemisinin resistance is defined as slow clearance post drug exposure as measured by a ring-stage survival assay (RSA) (31). We tested TDI4258 in combination with DHA using a modified ring-stage survival assay (RSA) with artemisinin-resistant parasites that contain a mutant Kelch (R539T) protein in a multidrug-resistant Dd2 strain background (32). We exposed early 1- to 3-h ring-stage parasites to a 3-h pulse of DHA and continuous TDI4258 for 72 h, as described (5, 31). Parasitemia was measured at 72 h post initial exposure. Isobologram analysis demonstrated synergistic killing of artemisinin-resistant parasites by the combination of TDI4258 and DHA (Fig. 5*A*). Wild-type Dd2 parasites remained sensitive to DHA and thus could not be assessed for synergy in this assay.

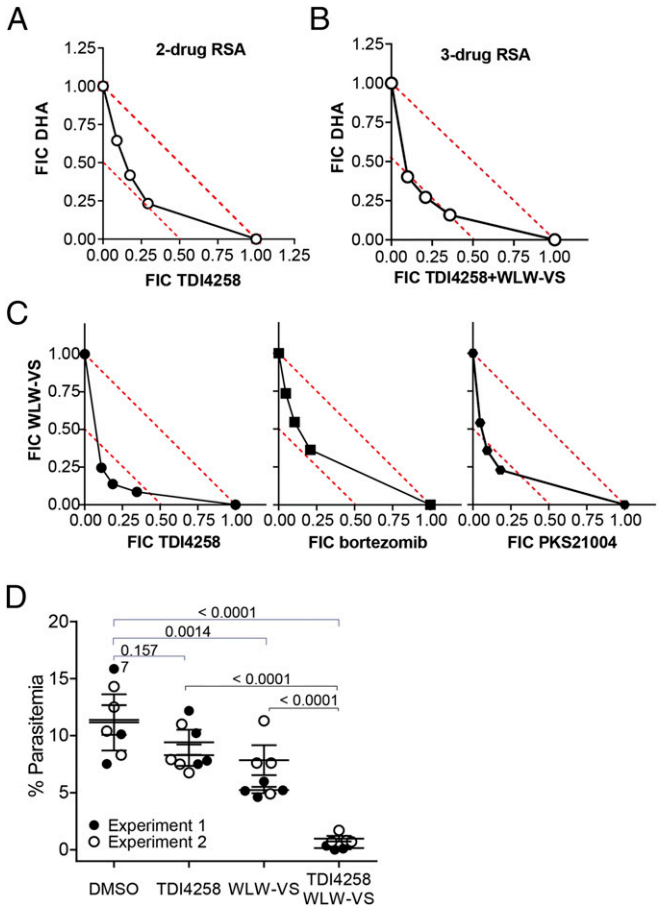

Fig. 5. In vitro synergy of AsnEDA and DHA, between β5 and β2 inhibition and in vivo enhancement of anti-*P. yoelii* activity in a mouse model of malarial infection. (*A*) In vitro synergy of TDI4258 and DHA against artemisinin-resistant *P. falciparum* Dd2 Kelch13$_{R539T}$. (*B*) In vitro synergy between the combination of TDI4258, WLW-VS, and DHA against artemisinin-resistant *P. falciparum* Dd2 Kelch13$_{R539T}$. (*C*) FIC values were determined for pairs TDI4258/WLW-VS, bortezomib/WLW-VS, and PKS21004/WLW-VS using a 72-h dual drug assay. (*D*) In vivo activity against *P. yoelii* in female CF1 mice. The percentage of parasitemia was calculated by microscopic analysis of Giemsa-stained blood smear samples at 5 d postinfection. The experiments were repeated twice and are shown by filled and open circles, respectively. Mean parasitemia and statistical significance were calculated using pooled data. A one-way ANOVA test was used for statistical analysis; $n = 4$ mice per group.

Synergistic in Vitro Activity Against *P. falciparum* of Proteasome Inhibitors That Target β2 and β5 Pf20S Subunits. To test if the synergy we noted above between β2 and β5 inhibitors against Pf20S pertained to intact parasites, we tested β5 inhibitors together with various concentrations of WLW-VS against the erythrocytic stages of *P. falciparum* as described (33) and determined the viability of intraerythrocytic parasites at 72 h. PKS21004, TDI4258, and bortezomib all gave fractional inhibition concentration (FIC) values of ≤0.5, demonstrating a synergistic effect of simultaneous inhibition of Pf20S β5 and β2 (Fig. 5*C*). This suggests that the binding of a ligand to one subunit can affect the binding of another ligand to a distal subunit of the Pf20S.

Next we tested combined inhibition of P20S β2 and β5 (in a fixed ratio of TDI4258:WLW-VS of 4:1) in the presence of DHA in a ring-stage survival assay with an artemisinin-resistant strain, as described above. Potent synergy after 3 h exposure to the compounds was evident when viability was assessed 72 h after initial exposure (Fig. 5*B*).

In Vivo Antimalarial Activity. The in vivo efficacy of TDI4258 was tested in a mouse model of *Plasmodium yoelii* infection. Female CF1 mice were infected i.v. with 3×10^5 *P. yoelii*-parasitized erythrocytes and were treated daily for 4 d beginning 1 d after inoculation. TDI4258 (15 mg/kg), WLW-VS (60 mg/kg), and WLW-VS (60 mg/kg) plus TDI4258 (15 mg/kg) were administered i.p. in DMSO. Parasitemia was determined on day 5. The experiment was performed twice, and the data were pooled (Fig. 5*D*). TDI4258 did not yield a statistically significant reduction in parasitemia compared with DMSO (21.5% reduction, $P = 0.16$), likely reflecting its short (30-min) half-life in the mouse (*SI Appendix*, Table S2). WLW-VS reduced parasitemia by 42% ($P = 0.0014$). The combination of TDI4258 and WLW-VS reduced parasitemia by 95% ($P < 0.0001$). Thus, the synergy observed in vitro between inhibition of P20S β2 and β5 appeared to manifest in vivo during murine *P. yoelii* infection.

Mechanism of Resistance. For additional target validation and to explore potential mechanisms of resistance, we cultured the Dd2 strain of *P. falciparum* parasites in gradually increasing concentrations of PKS21004 from the initial EC_{50} of 4 nM to 192 nM. After 4 mo, we obtained a stably resistant parasite line. We were not able to generate any resistant parasites using the same protocol with 3D7-strain parasites. We cloned parasites from the resistant Dd2 line and maintained two clonal lines, *P. falciparum* Dd2-R1 and Dd2-R2. Both demonstrated ∼130-fold resistance to PKS21004 (Fig. 6*A*). Resistance extended to other members of the AsnEDA class; for example, both lines were 40-fold more resistant to PKS21224 and 13-fold more resistant to TDI4258 than unselected Dd2 parasites. However, resistance was specific, in that there was little or no change in EC_{50}s against DHA, atovaquone, or piperaquine (Fig. 6*A*).

Intriguingly, the AsnEDA-resistant parasites did not demonstrate resistance to another β5 inhibitor, bortezomib; on the contrary, they demonstrated a twofold increase in susceptibility to bortezomib. Bortezomib is a dipeptide boronate that forms a reversible covalent boron–oxygen bond with the hydroxyl group of the active site Thr^{1N} and primarily targets the β5 subunit (34). Its P1 Leu and P2 Phe side chains bind to S1 and S2 pockets, respectively, and its pyrazinoyl moiety binds along the substrate-binding groove (35). The mutation conferring resistance to the AsnEDA β5 inhibitors slightly enhanced the action of a dipeptidyl boronate with a different binding pose. Increased sensitivity was also seen with carfilzomib, a peptide epoxyketone proteasome inhibitor drug. Moreover, the AsnEDA-resistant parasites had 12- to 14-fold increased sensitivity to the β2 inhibitor WLW-VS.

To gain insight into the mechanism of resistance, we sequenced the genomes of the parental Dd2 strain and the two resistant clones, *P. falciparum* Dd2-R1 and Dd2-R2. Surprisingly,

A

EC50s and fold changes in EC50s compounds against Pf Dd2, Pf Dd2-R1 and -R2 resistant strains

		EC50 (nM) (fold of change in EC50)		
		Pf Dd2	Pf Dd2-R1	Pf Dd2-R2
Proteasome inhibitors	PKS21004	2.5	326 (130)	345 (138)
	PKS21224	39.2	1548 (40)	1618 (41)
	TDI4258	27.6	279 (10)	349 (13)
	Bortezomib	257	106 (0.4)	130 (0.5)
	Carfilzomib	21.7	17.5 (0.8)	21.8 (0)
	WLW-VS*	119.7	7.3 (0.07)	9.7 (0.08)
Antimalarial drugs	DHA	2.0	1.2 (0.6)	1.7 (0.9)
	Piperaquine	25.5	28.1 (1.1)	18.9 (0.7)
	Atovaquone	1.9	3.4 (1.8)	2.1 (1.1)

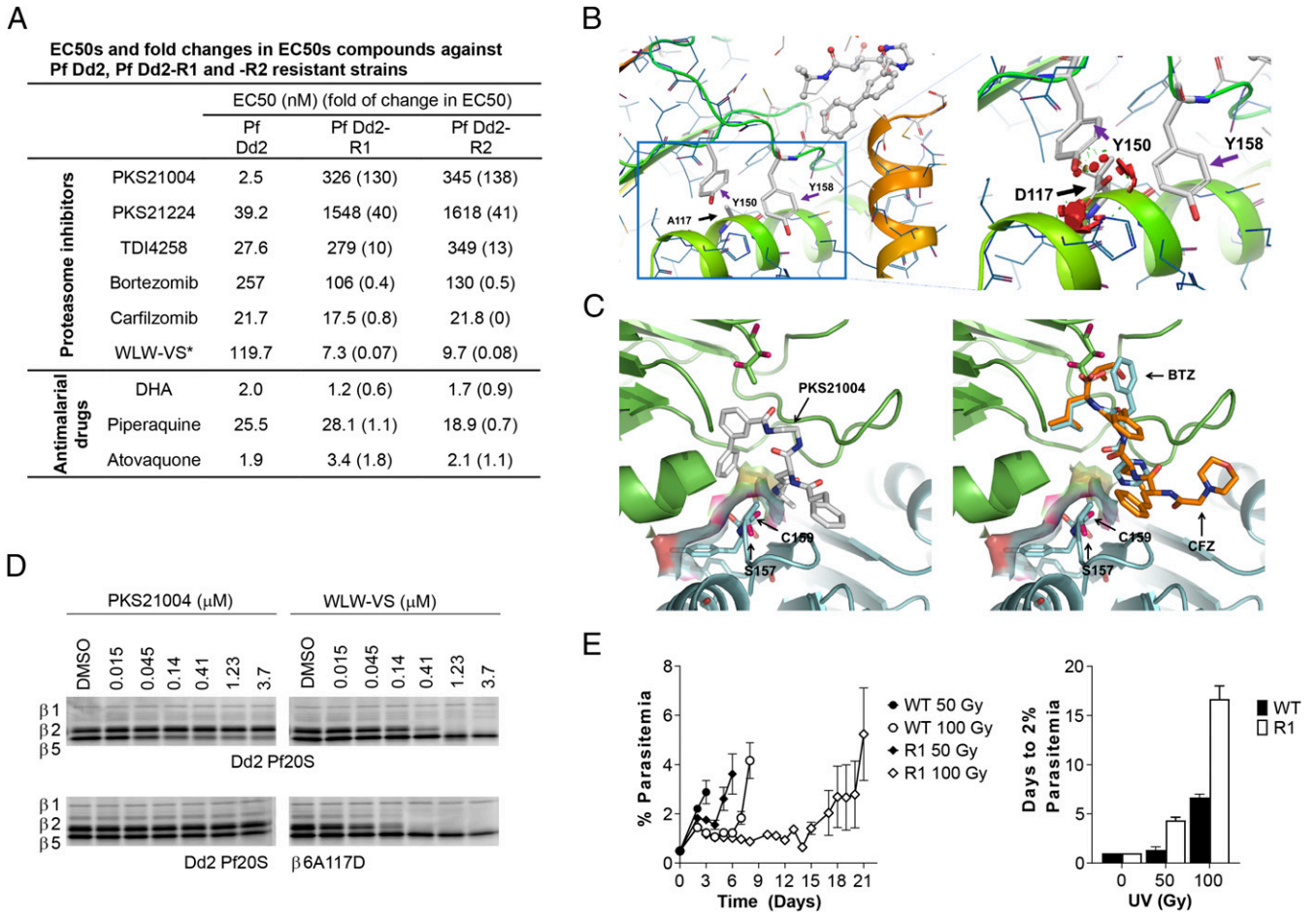

Fig. 6. AsnEDA resistance. (*A*) EC_{50}s for parental Dd2 and two clonal resistant parasite lines. Resistant parasites had increased sensitivity to the β2 inhibitor WLW-VS and to the β5 inhibitors bortezomib and carfilzomib, with no change in EC_{50}s of unrelated antimalarials. (*B*) Computational mutation of β6 A117 to aspartate. A117 is surrounded by β6 Y150 and Y158 with the shortest distance of 3.5 Å and 3.8 Å between the side chain residue of A117/Y150 and A117/Y158, respectively. With the mutation of A117D, both rotamers lead to a steric clash between the charged side chain of D117 with Y150 and with Y158, respectively (highlighted in red). (*C*) Superimposition of Pf20S β5β6 with PKS21004 (*Left*) and with bortezomib (BTZ) and carfilzomib (CFZ) (*Right*). The A117D mutation forces conformational changes in the S1SP and S3 pockets, with which PKS21004 interacts, whereas bortezomib and carfilzomib do not interact. (*D*) Inhibition of Pf20S (*Upper*) and Pf20S(β6A117D) (*Lower*) by PKS21004 (*Left*) and WLW-VS (*Right*), assessed by MV151. (*E*) Trophozoite-stage cultures at 0.5% parasitemia were irradiated at 50 and 100 Gy. (*Left*) Parasite growth was monitored daily. A representative experiment done in triplicate is shown. (*Right*) R1 parasites irradiated with 50 or 100 Gy took 4.3 and 16.7 d to recover growth, respectively, compared with Dd2 that took 1.3 and 6.8 d, respectively. The data are the means from two independent experiments, each performed in triplicate.

as summarized in *SI Appendix*, Table S6, both resistant clones bear a G-to-A mutation in the gene encoding the β6 proteasome subunit (PF3D7_0518300), leading to an A117D amino acid change; no mutation was found in the target β5 subunit. Both clonal lines also harbored mutations in PF3D7_0822400, a gene of unknown function (*SI Appendix*, Table S6). One clone also carried a mutation in PF3D7_0724700, which encodes another protein of unknown function. There was no evidence of copy number variation of any genes.

The β6 proteasome subunit has no proteolytic activity. A117 is predicted to reside in an α-helix adjacent to a loop (Tyr152–Cyc159), part of which forms a wall between the β5 S1 side pocket (S1SP) and the β5 S3 pocket. A117 is closely opposed to β6 Tyr150 and β6 Tyr158, whose side chains are only 3.4 and 3.7 Å distant from A117, respectively (Fig. 6*B*). The A117D mutation introduces a negatively charged side chain that is expected to clash with these two tyrosines (Fig. 6*B*), forcing the loop to undergo conformational changes that would alter the shape and polarity of the S1SP and the S3 pocket in β5, directly affecting the binding of PKS21004. In contrast, the A117D and accompanying conformational changes are distal to the binding sites of both bortezomib and carfilzomib (Fig. 6*C*), potentially explaining why the mutant was not resistant to both bortezomib and carfilzomib.

To confirm that the mutation affected the binding affinity of PKS21004, we enriched mutant Pf20S(β6A117D) and conducted subunit labeling experiments (Fig. 6*D*, *Left*). In agreement with the shift in EC_{50}, PKS21004's potency in blocking the labeling of Pf20S β5 in Pf20S(β6A117D) by MV151 was reduced compared with its ability to block the labeling of the wild-type proteasome. Conversely, the potency of WLW-VS in blocking the labeling of Pf20Sβ2 by MV151 was greater in the mutant than in the wild type (Fig. 6*D*, *Right*).

Drug resistance-mediating mutations may be accompanied by loss of fitness (36). To test if the β6 A117D mutation imposed a fitness cost, we performed a plaque assay comparing the Pf Dd2 parent with the Pf Dd2 R1 parasite line and identified subtle (37) but significant differences in growth rates under normal culture conditions, with the Pf Dd2 parent appearing to have more robust growth than the resistant parasite line (*SI Appendix*, Fig. S6). We then exposed intraerythrocytic *P. falciparum* to X-ray irradiation at 50 and 100 Gy, which is likely to damage DNA and protein, and measured the parasite's ability to recover from this

stress by monitoring the recovery of parasitemia to 2% (Fig. 6*E*, *Left*) (38). Pf Dd2 recovered by days 1.3 (after 50 Gy) and 6.8 (after 100 Gy), whereas PfDd2 R1 recovered by days 4.3 (50 Gy) and 16.7 (100 Gy) (Fig. 6*E*, *Right*), demonstrating a defect in the ability of the resistant parasite line to withstand radiation stress.

Discussion

The spread of drug-resistant parasites is a major obstacle to the WHO's goal of reducing morbidity and mortality attributable to malaria by 90% by 2030. Here we present a set of compounds that spare both human constitutive and immuno-proteasomes and target the malaria parasite proteasome. The proteasome is a key regulator of the parasite's ability to proliferate and adapt to stress, likely including stresses imposed by artemisinin antimalarials (5). We show that simultaneously targeting two different catalytic proteasome subunits provides synergistic killing of *P. falciparum* as well as synergism with artemisinin against artemisinin-resistant parasites. Moreover, a mutation in the parasite proteasome that confers resistance to blockade of one subunit can lead to increased sensitivity to blockade of another. These results suggest that, despite the conservation of proteasomes among eukaryotes, targeting *P. falciparum* proteasome subunits offers a more promising approach for antimalarial chemotherapy than was previously apparent.

We determined the activity of the AsnEDAs at multiple stages of the malaria lifecycle. Activity against the gametocyte stage has previously been determined only with nonselective inhibitors. Here we found that the relatively selective AsnEDAs were effective against stage III and stage V gametocytes, the stage poised for transmission to the mosquito. The AsnEDAs also blocked male gamete activation, supporting the idea that proteasome inhibitors can act as transmission-blocking antimalarials at several stages. Our studies on the liver stage are unique in that the species-selective nature of the compounds allowed us to treat intrahepatic parasites for a prolonged time without toxicity to the host cell. The efficacy of AsnEDAs at the preerythrocytic stage indicates the potential use of proteasome inhibitors for malaria prevention. This observation opens the door to study the biology of the parasite proteasome in this important stage, which is associated with extensive parasite remodeling (30).

The availability of cryo-EM structures (17) to guide modeling studies helped us better understand and improve the selectivity of inhibitors for the *P. falciparum* proteasome against both the human constitutive proteasome and immunoproteasome. Expression of human c-20S is ubiquitous, while i-20S is expressed predominantly in immune cells and proportionately more so when they are stimulated with IFN-γ. The immunoproteasome plays important roles in the activation of immune cells and in immune surveillance. Selectivity for the pathogen's proteasome is crucial for proteasome inhibitors to advance as antiinfective agents.

Resistance to AsnEDA β5 inhibitors emerged in vitro only after prolonged in vitro selection in one of two *P. falciparum* lines tested. The resistance was associated with a mutation not in the target β5 subunit but in the adjacent β6 noncatalytic structural subunit. Modeling studies suggest that the amino acid change in β6 may alter the S1SP and S3 pockets formed by β5 and β6. This demonstrates that a mutation in the β6 subunit confers resistance to Pf20S β5 inhibitors by affecting distal region of the substrate binding cleft. Similarly, a single amino acid mutation in the trypanosomal proteasome nonproteolytic β4 subunit conferred resistance to a newly identified kinetoplastid-specific proteasome inhibitor (20). The additional mutation in PF3D7_0822400, a conserved protein with no known function, may contribute to resistance to proteasome inhibitors; a supportive or adaptive role for this mutation has yet to be explored.

The efficacy of AsnEDAs and WLW-VS with cultured parasites and in murine malaria infection suggests that combination therapy with inhibitors of both the *Plasmodium* Pf20S β5 and β2 subunits could offer an effective therapy for malaria, provided that ongoing medicinal chemistry efforts lead to improved oral bioavailability. Targeting both these subunits was synergistic against purified proteasomes, erythrocytic-stage parasites in vitro, and erythrocytic-stage parasites in the mouse. Similarly, enhanced cytotoxicity from combined inhibition of the β2 and β5 subunits has been described in human tumor cells (39, 40). The findings reported here provide a biologic rationale for medicinal chemistry campaigns directed at both subunits and suggest that it will be fruitful to consider each set of inhibitors in the context of its interaction with others. In addition, given that resistance to a β5 inhibitor led to increased sensitivity to a β2 inhibitor both in enzymatic studies and in vitro culture, dual inhibition appears to lead to a highly desirable resistance-thwarting strategy, collateral sensitivity (41). Further structural studies with wild-type and A117D-mutant strains of Pf20S, with and without inhibitors, should shed light on the mechanism driving the increased sensitivity to WLW-VS observed in PKS21004-resistant parasites.

A fitness cost that accompanies the development of drug resistance has been described for various microorganisms, including *P. falciparum*, and can help limit the spread of drug-resistant parasites. Similarly, yeast bearing mutations associated with bortezomib resistance grew more slowly than wild type, especially under stress conditions (42). The majority of mutations reported to confer resistance to proteasome inhibitors in yeast or cancer cells are in β5, in contrast to the β6 mutation we identified in each of two resistant lines of *P. falciparum*.

The present findings strengthen the case for targeting the parasite proteasome in antimalarial drug development. The inhibitors described demonstrate the potential to inhibit the *P. falciparum* proteasome while sparing not only the human constitutive proteasome but also the human immunoproteasome. Further, they show that inhibition of the *P. falciparum* β5 subunit can kill or block parasite development in all stages of the parasite lifecycle—in the asexual blood stage, during hepatic invasion and development, and in the development and activation of gametocytes—offering the potential for chemoprevention (by killing liver stages) and transmission blocking (by inhibiting gametocytes and gamete activation), stages for which there are few active antimalarials. Finally, these compounds revealed the synergistic potential of exploiting long-range interactions between distinct proteolytic subunits of Pf20S as well as the opportunity for collateral sensitivity. Further development of parasite proteasome inhibitors will be aided by a deeper understanding of the complex relationships among the proteasome subunits. Such an understanding may be translated clinically to maximize potency and raise the barrier to the development of resistance.

Materials and Methods

The *SI Appendix, SI Methods* details materials and methods for *P. falciparum* cultivation; Pf20S enrichment; biochemical characterization of Pf20S; IC_{50} determinations against c-20S, i-20S, and Pf20S; dose–response studies against parasites in erythrocytic, preerythrocytic, and gametocyte asexual stages and against gamete activation; selection of resistant mutants; active subunit labeling; PRR assay; efficacy studies in mice; molecular modeling; assays for synergy, plaque formation, and recovery from irradiation; chemical synthesis; and characterization of compounds. In vivo efficacy studies were performed with the approval of the Portland Veterans Administration Medical Center Institutional Animal Care and Use Committee. The relevant clinical trials and analyses of cultured parasites were approved by the Uganda National Council of Science and Technology, the Makerere University Research and Ethics Committee, and the University of California, San Francisco Committee on Human Research. Informed consent was obtained from the blood sample donors.

ACKNOWLEDGMENTS. We thank Takeda Pharmaceuticals, Inc. for providing pharmacokinetic analyses and GlaxoSmithKline's Diseases of the Developing World campus at Tres Cantos, Spain for providing gamete activation and pharmacokinetic assays as gifts-in-kind; Dr. Takafumi Yukawa, Dr. Akinori

Toita, Mr. Tzu-Tshin Wong, Dr. John Ginn, Dr. Andrew Stamford, and Dr. Peter Meinke at Tri-Institutional Therapeutics Discovery for medicinal chemistry discussions; Dr. J. David Warren at The Abby and Howard P. Milstein Synthetic Chemistry Core Facility at Weill Cornell Medicine for assistance; Dr. Hao Li and Dr. Matthew Bogyo for advice and sharing reagents; Ms. Stephanie A. Rasmussen (Dominican University) and Amanda Chan (Weill Cornell Medicine) for technical assistance; Jamie Bean (Memorial Sloan Kettering Cancer Center, MSKCC) for assistance with whole-genome sequencing; Dr. Angelika Sturm, Dr. Koen Dechering, and Mr Rob Henderson at TropIQ Health Sciences for providing parasite biomass; and Dr. Katja Becker at Justus Liebig University Giessen for sharing reagents. This work was supported by NIH Grants 1R21AI123794 (to G.L. and L.A.K.), R21 AI101393 (to G.L.), 1R21AI094167 (to P.B.), AI075045 (to P.J.R. and R.A.C.), and T37MD003407 (to L.F.G. and D.J.M.); National Science Foundation Grant IOS-1146221 (to P.B.); the Department of Medicine, Weill Cornell Medicine Seed Fund (L.A.K.); the Tri-Institutional Therapeutics Discovery Institute and Weill Cornell Medicine Matching Fund (G.L.); Medicines for Malaria Venture RD/15/0001 (R.A.C. and P.J.R.); and United States Department of Veterans Affairs Biomedical Laboratory Research and Development Grant BX002440 (to J.S.D.). We acknowledge the use of the Integrated Genomics Operation Core at MSKCC, funded by the National Cancer Institute Cancer Center Support Grant P30 CA08748, Cycle for Survival, and the Marie-Josée and Henry R. Kravis Center for Molecular Oncology (MSKCC). The Department of Microbiology and Immunology at Weill Cornell Medicine is supported by the William Randolph Hearst Trust. L.A.K. is a Hearst Clinical Scholar.

1. WHO (2016) *World Malaria Report 2016* (WHO, Geneva).
2. Ariey F, et al. (2014) A molecular marker of artemisinin-resistant *Plasmodium falciparum* malaria. *Nature* 505:50–55.
3. Mbengue A, et al. (2015) A molecular mechanism of artemisinin resistance in *Plasmodium falciparum* malaria. *Nature* 520:683–687.
4. Imwong M, Hien TT, Thuy-Nhien NT, Dondorp AM, White NJ (2017) Spread of a single multidrug resistant malaria parasite lineage (PfPailin) to Vietnam. *Lancet Infect Dis* 17:1022–1023.
5. Dogovski C, et al. (2015) Targeting the cell stress response of *Plasmodium falciparum* to overcome artemisinin resistance. *PLoS Biol* 13:e1002132.
6. Li H, et al. (2016) Structure- and function-based design of Plasmodium-selective proteasome inhibitors. *Nature* 530:233–236.
7. Li H, et al. (2014) Assessing subunit dependency of the Plasmodium proteasome using small molecule inhibitors and active site probes. *ACS Chem Biol* 9:1869–1876.
8. Li H, et al. (2014) Identification of potent and selective non-covalent inhibitors of the *Plasmodium falciparum* proteasome. *J Am Chem Soc* 136:13562–13565.
9. Li H, et al. (2012) Validation of the proteasome as a therapeutic target in Plasmodium using an epoxyketone inhibitor with parasite-specific toxicity. *Chem Biol* 19: 1535–1545.
10. LaMonte GM, et al. (2017) Development of a potent inhibitor of the Plasmodium proteasome with reduced mammalian toxicity. *J Med Chem* 60:6721–6732.
11. Gantt SM, et al. (1998) Proteasome inhibitors block development of Plasmodium spp. *Antimicrob Agents Chemother* 42:2731–2738.
12. Lindenthal C, Weich N, Chia YS, Heussler V, Klinkert MQ (2005) The proteasome inhibitor MLN-273 blocks exoerythrocytic and erythrocytic development of Plasmodium parasites. *Parasitology* 131:37–44.
13. Kreidenweiss A, Kremsner PG, Mordmüller B (2008) Comprehensive study of proteasome inhibitors against *Plasmodium falciparum* laboratory strains and field isolates from Gabon. *Malar J* 7:187.
14. Czesny B, Goshu S, Cook JL, Williamson KC (2009) The proteasome inhibitor epoxomicin has potent *Plasmodium falciparum* gametocytocidal activity. *Antimicrob Agents Chemother* 53:4080–4085.
15. Aminake MN, et al. (2011) Thiostrepton and derivatives exhibit antimalarial and gametocytocidal activity by dually targeting parasite proteasome and apicoplast. *Antimicrob Agents Chemother* 55:1338–1348.
16. Muchamuel T, et al. (2009) A selective inhibitor of the immunoproteasome subunit LMP7 blocks cytokine production and attenuates progression of experimental arthritis. *Nat Med* 15:781–787.
17. Santos RLA, et al. (2017) Structure of human immunoproteasome with a reversible and noncompetitive inhibitor that selectively inhibits activated lymphocytes. *Nat Commun* 8:1692.
18. Lin G, et al. (2009) Inhibitors selective for mycobacterial versus human proteasomes. *Nature* 461:621–626.
19. Lin G, et al. (2013) N,C-Capped dipeptides with selectivity for mycobacterial proteasome over human proteasomes: Role of S3 and S1 binding pockets. *J Am Chem Soc* 135:9968–9971.
20. Khare S, et al. (2016) Proteasome inhibition for treatment of leishmaniasis, Chagas disease and sleeping sickness. *Nature* 537:229–233.
21. Hsu HC, et al. (2017) Structural basis for the species-selective binding of N,C-capped dipeptides to the *Mycobacterium tuberculosis* proteasome. *Biochemistry* 56:324–333.
22. Sula Karreci E, et al. (2016) Brief treatment with a highly selective immunoproteasome inhibitor promotes long-term cardiac allograft acceptance in mice. *Proc Natl Acad Sci USA* 113:E8425–E8432.
23. Singh PK, et al. (2016) Immunoproteasome beta5i-selective dipeptidomimetic inhibitors. *ChemMedChem* 11:2127–2131.
24. Fan H, Angelo NG, Warren JD, Nathan CF, Lin G (2014) Oxathiazolones selectively inhibit the human immunoproteasome over the donstitutive proteasome. *ACS Med Chem Lett* 5:405–410.
25. Smilkstein M, Sriwilaijaroen N, Kelly JX, Wilairat P, Riscoe M (2004) Simple and inexpensive fluorescence-based technique for high-throughput antimalarial drug screening. *Antimicrob Agents Chemother* 48:1803–1806.
26. Verdoes M, et al. (2006) A fluorescent broad-spectrum proteasome inhibitor for labeling proteasomes in vitro and in vivo. *Chem Biol* 13:1217–1226.
27. Rasmussen SA, et al. (2017) Changing antimalarial drug sensitivities in Uganda. *Antimicrob Agents Chemother* 61:e01516-17.
28. Sanz LM, et al. (2012) P. falciparum in vitro killing rates allow to discriminate between different antimalarial mode-of-action. *PLoS One* 7:e30949.
29. Miguel-Blanco C, et al. (2017) Hundreds of dual-stage antimalarial molecules discovered by a functional gametocyte screen. *Nat Commun* 8:15160.
30. Govindasamy K, et al. (2016) Invasion of hepatocytes by Plasmodium sporozoites requires cGMP-dependent protein kinase and calcium dependent protein kinase 4. *Mol Microbiol* 102:349–363.
31. Witkowski B, et al. (2013) Novel phenotypic assays for the detection of artemisinin-resistant *Plasmodium falciparum* malaria in Cambodia: In-vitro and ex-vivo drug-response studies. *Lancet Infect Dis* 13:1043–1049.
32. Straimer J, et al. (2015) Drug resistance. K13-propeller mutations confer artemisinin resistance in *Plasmodium falciparum* clinical isolates. *Science* 347:428–431.
33. Gorka AP, Jacobs LM, Roepe PD (2013) Cytostatic versus cytocidal profiling of quinoline drug combinations via modified fixed-ratio isobologram analysis. *Malar J* 12: 332.
34. Groll M, Berkers CR, Ploegh HL, Ovaa H (2006) Crystal structure of the boronic acid-based proteasome inhibitor bortezomib in complex with the yeast 20S proteasome. *Structure* 14:451–456.
35. Schrader J, et al. (2016) The inhibition mechanism of human 20S proteasomes enables next-generation inhibitor design. *Science* 353:594–598.
36. Rosenthal PJ (2013) The interplay between drug resistance and fitness in malaria parasites. *Mol Microbiol* 89:1025–1038.
37. Thomas JA, et al. (2016) Development and application of a simple plaque assay for the human malaria parasite *Plasmodium falciparum*. *PLoS One* 11:e0157873.
38. Calhoun SF, et al. (2017) Chromosome end repair and genome stability in *Plasmodium falciparum*. *MBio* 8:e00547-17.
39. Weyburne ES, et al. (2017) Inhibition of the proteasome beta2 site sensitizes triple-negative breast cancer cells to beta5 inhibitors and suppresses Nrf1 activation. *Cell Chem Biol* 24:218–230.
40. Kraus M, et al. (2015) The novel β2-selective proteasome inhibitor LU-102 synergizes with bortezomib and carfilzomib to overcome proteasome inhibitor resistance of myeloma cells. *Haematologica* 100:1350–1360.
41. Baym M, Stone LK, Kishony R (2016) Multidrug evolutionary strategies to reverse antibiotic resistance. *Science* 351:aad3292.
42. Huber EM, Heinemeyer W, Groll M (2015) Bortezomib-resistant mutant proteasomes: Structural and biochemical evaluation with carfilzomib and ONX 0914. *Structure* 23: 407–417.